Superconductivity of Mg/MgO interface formed by shock-wave pressure

N. S. Sidorov,[1] A. V. Palnichenko,[1] D. V. Shakhrai,[2] V. V. Avdonin,[2] O. M. Vyaselev,[1] and S. S. Khasanov[1]

[1]*Institute of Solid State Physics, Russian Academy of Sciences, Chernogolovka, Moscow region, 142432, Russia*
[2]*Institute of Problems of Chemical Physics, Russian Academy of Sciences, Chernogolovka, Moscow region, 142432, Russia*
(Dated: March 29, 2013)

A mixture of Mg and MgO has been subjected to a shock-wave pressure of $\simeq 170$ kbar. The ac susceptibility measurements of the product has revealed a metastable superconductivity with $T_c \approx 30$ K, characterized by glassy dynamics of the shielding currents below T_c. Comparison of the ac susceptibility and the dc magnetization measurements infers that the superconductivity arises within the interfacial layer formed between metallic Mg and its oxide due to the shock-wave treatment.

I. INTRODUCTION

Interfacial superconductivity is one of the emergent phenomena that appears at the boundary between some materials, even insulators, as a consequence of a large change of physical properties of these materials at the interface, compared to their properties in the bulk.[1–3] It has been experimentally evidenced since the 1950's and 60's that specifically fabricated thin layers of some superconductors (e.g. sputtered onto a cold substrate of sandwiched between non-superconducting materials) demonstrate a higher superconducting transition temperature, T_c, compared to that in the bulk.[4–9] However, it took several decades before the necessary technologies providing wide abilities of fabricating two-dimensional heterostructures controlled on the molecular and atomic scale were developed, which enabled the creation of many novel materials on the basis of interfaces.[10,11]

The superconducting interfaces known currently, belong to the families of semiconductor/semiconductor interfaces based on different chalcogenides,[12–15] insulator/insulator interfaces based on LaAlO$_3$/SrTiO$_3$ and related systems,[16,17] as well as metal/insulator interfaces based on complex oxides such as La$_{1.55}$Sr$_{0.45}$CuO$_4$/La$_2$CuO$_4$.[18] The origin of the interfacial superconductivity is not completely understood yet. Moreover, there are only few examples of the interfacial superconducting layer with T_c higher than in the bulk optimally doped samples.[2] The complexity of the used oxides makes the issue even more obscure. Therefore, discovery of superconducting interfaces formed by simplest non-superconducting substances could illuminate the issue by revealing the key factors responsible for the interface superconductivity.

Mg/MgO system formed by thermal surface oxidation of bulk metallic Mg samples, is one of the first of such elementary systems where the interface between non-superconducting constituents has been reported to superconduct at 39-54 K.[19,20] Historically, this experiment was motivated by earlier efforts to increase $T_c = 39$ K in magnesium diboride, MgB$_2$, by heating it in the presence of alkali metals. The efforts failed for pure MgB$_2$,

but resulted in T_c up to 45-58 K for the mixture of MgB$_2$ and MgO,[21] which was attributed to metal/metal oxide interfaces formed by alkali metal chemical reduction of MgO inclusions. The above experiments have shown also an instability of the superconducting Mg/MgO-interface at room temperature. Superconductivity of a Mg/MgO sample, vacuum-encapsulated in quartz ampoule, decays gradually during its exposure to room temperature, while storing the ampoule in liquid nitrogen prevents the sample degradation infinitely long. This suggests the importance to quench the non-equilibrium sample to low temperature in order to stabilize the superconducting Mg/MgO-interface.[19,20]

Such instability of the non-equilibrium superconducting Mg/MgO-interface under normal conditions has motivated our attempt to create it using shock-wave pressure. During the shock-wave impact, a stroke applied to the sample creates a series of strong high-pressure shock-waves propagating throughout the sample due to relative displacements of local parts of the sample material.[22–24] Highly non-equilibrium conditions thus realized, can stimulate phase transitions or mechanochemical reactions inaccessible in a static pressure mode.[25,26] Furthermore, the energy of the shock wave rapidly propagating through the sample within 10^{-6} – 10^{-9} s,[22–25] leads to local non-equilibrium overheat of the sample's regions at the shock wavefront, followed by their rapid cooling (quenching) as the shock-wave is passed. Such quenching can provide room-temperature stabilization of metastable non-equilibrium phases, unstable otherwise under normal conditions.

In this paper we report on metastable superconductivity at ≈ 30 K revealed by the ac magnetic susceptibility measurements of the mixture of Mg and MgO subjected to shock-wave pressure of $\simeq 170$ kbar.

II. EXPERIMENTAL

A. Sample preparation

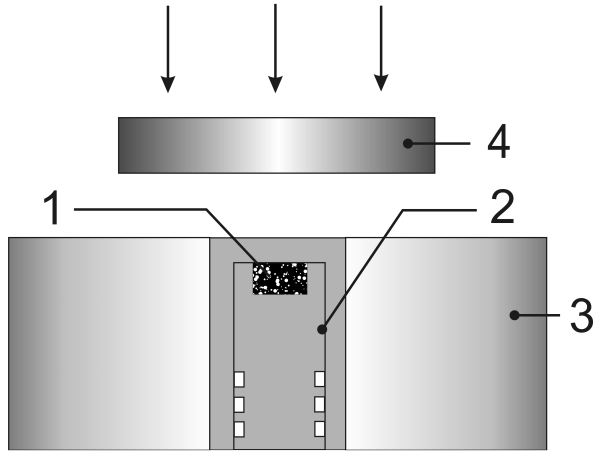The samples were prepared using flat-type shock-wave pressure setup, machined of X18H10 stainless steel, de-

FIG. 1: Layout of the shock-wave pressure setup. (1) - sample, (2) - conservation cell, (3) - guard ring, (4) - impactor.
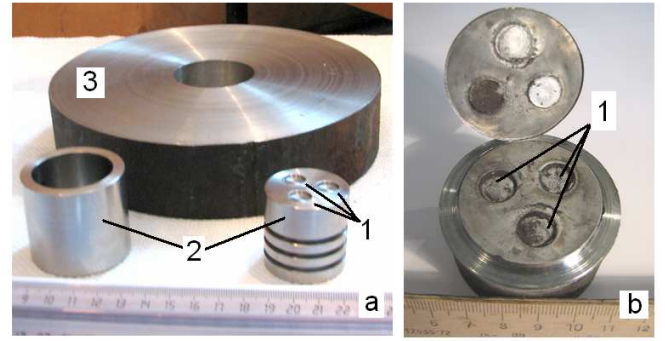

FIG. 2: Photographs of the unassembled virgin shock-wave pressure setup (a) and cut-open conservation cell after the shock-wave impact (samples extracted) (b). (1) - sample wells, (2) - conservation cell, (3) - guard ring.

scribed earlier in Refs. 25,26. The starting samples were tablets, 9.6 mm in diameter and 0.9 mm thick, prepared of 99.99 %-pure metallic magnesium covered by 0.2 mm layer of powdered, 10 - 50 μm grain size, 99.99 %-pure magnesium oxide, MgO. Prior to the shock-wave pressure treatment, the samples were compacted to reduce porosity using static pressure up to 0.3 kbar.

Layout of the shock-wave pressure setup is shown in Fig. 1. Compacted sample (1) reside in conservation cell (2) placed inside guard ring (3). Aluminum impactor (4) accelerated up to 1.05 km/s by explosion products hits the cell lid. During the impact, the pressure is monitored by manganin pressure gauges, whereas the average temperature of the sample is estimated by P–V–T state equations of MgO and Mg.[27,28]

Within microseconds, the impact generates in the sample a series of consecutive planar shock-waves of pressure.[25] Due to energy dissipation processes in the shock-wave, the sample is heated. The heating is controlled by adjusting the shock-wave setup. For preparing the superconducting Mg/MgO-samples, the optimum value of the shock-wave pressure, within 1 Mbar range, was found 170 kbar, which corresponds to an upper estimate of 340 K for the average temperature of the sample.

After the shock-wave pressure treatment, the conservation cell was cut open and the samples were extracted. The photographs of the shock-wave setup before and after the impact are shown in Fig. 2. The extracted samples were vacuum-encapsulated into 5 cm-long quartz ampoules having 0.9 mm-thick walls and 6 mm outer diameter, and stored in liquid nitrogen to prevent their degradation under normal conditions.

B. Measurements

The samples were studied by measuring the dynamic magnetic susceptibility, $\chi = \chi' - i\chi''$, using a mutual inductance ac susceptometer,[29] mounted inside a variable temperature insert. To avoid sample degradation, the measurements were done without unsealing the ampoules. The ampoule with the sample was placed inside one of the two identical pick-up coils positioned coaxially inside a long excitation coil that provided a uniform ac drive magnetic field at the sample position. ac voltage induced in the pick-up coils was fed to the differential input of a two-channel lock-in amplifier capable of segregating the in-phase,χ', and an out-of-phase, χ'', components of the ac susceptibility.The amplitude H_{ac} of the driving field ranged from 0.23 to 3.78 Oe, the driving frequency ν from 312 Hz to 20 kHz, and the superimposed dc magnetic field H_{dc} up to 170 Oe. The susceptometer was calibrated using ac susceptibility responses to the superconducting transitions in lead and niobium samples shaped similarly to the samples in study. An MgB$_2$ sample sealed in a similar quartz ampoule has shown the ac susceptibility response to the superconducting transition at 39 K, confirming correct thermometry of the measurement setup. The static magnetic moment of the Mg/MgO-sample sealed in the evacuated quartz ampoule was studied by SQUID magnetometer in the temperature range 5 - 70 K.

Crystal structure of the samples was investigated in the temperature range 80 – 300 K by X-ray diffraction measurements using Oxford Diffraction Gemini R diffractometer, MoK$_\alpha$ radiation, equipped with a cooling system that enables the measurements in the flow of cold nitrogen gas. For the diffraction measurements, the sample was extracted from the quartz ampoule in the ambience of liquid nitrogen and rapidly (within 5 -10 s) mounted onto the precooled goniometer of the diffractometer. Chemical composition of the samples was analyzed by energy dispersive X-ray microanalysis using Oxford INCA spectrometer.

III. EXPERIMENTAL RESULTS

Typical diffraction pattern of the shock-wave pressure treated Mg/MgO-sample recorded at $T = 80\,$K, is shown in Fig. 3. All the diffraction rings in the observed pattern are a superposition of the patterns from polycrystalline MgO ($a = 4.213\,$Å, space group Fm-3m) and Mg ($a = 3.209\,$Å, $c = 5.211\,$Å, space group P6$_3$/mmc) crystal structures.[30]
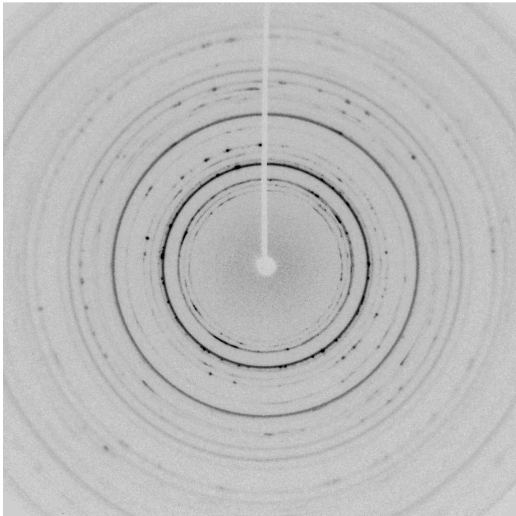

FIG. 3: X-ray diffraction pattern for the shock-wave pressure treated Mg/MgO-sample in MoK$_\alpha$ radiation. The complete diffraction ring set is a superposition of the patterns from polycrystalline MgO and Mg crystal structures.

Each cycle of χ measurements started from a cool-down of the Mg/MgO-sample to $4.2\,$K. Next, H_{ac} was switched on to enable the susceptibility measurements. These measurements at constant $T = 4.2\,$K have shown that χ decays monotonously in time t towards enlargement of diamagnetism, revealing a dynamics similar to spin glass behavior.[31] Curve 1 in Fig. 4 illustrates the $4\pi\chi'(t)$ dependence measured at frequency $\nu = 5.4\,$kHz at $H_{ac} = 0.6\,$Oe and $H_{dc} = 0$. $4\pi\chi'(t)$ was found to relax exponentially to a ground diamagnetic state as $a + b\exp(-t/\tau)$ (shown in Fig. 4 by a solid line) where a, b and τ are fit parameters. The fits to $\chi'(t)$ curves measured at frequencies from 0.312 to $20\,$kHz, give the same time constant $\tau = 19.9\,$min to within 1%.

After a one-hour ($\sim 3\tau$) delay at $T = 4.2\,$K, $\chi'(T)$ was measured upon heating at the rate of 1-1.5 K/min. No visible change of the measurement result was found with a slower heating rate. The measured $4\pi\chi'(T)$ is shown by Curve 1 in the Inset of Fig. 4. The drop in $4\pi\chi'(T)$ at $4.2\,$K corresponds to the decay of $\chi'(t)$, Curve 1 in Fig. 4. As the temperature increases, a step-like rise of $\chi'(T)$ is observed at $T_c = 29\,$K, signifying a phase transition in the sample at this temperature. In order to exclude the influence of the $\chi(t)$ relaxation processes on the $\chi(T)$ measurements, all subsequent $\chi(T)$ measurements were
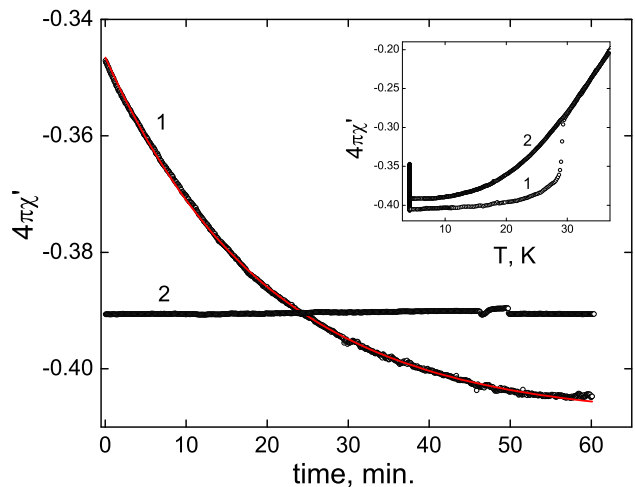

FIG. 4: Time evolution of $4\pi\chi'$ at $T = 4.2\,$K for the vacuum-encapsulated shock-wave treated Mg/MgO-sample (Curve 1) and for the same sample exposed to room temperature for 10 hours (Curve 2). Solid curve: fit to Curve 1 in the form $a + b\exp(-t/\tau)$, where a, b and τ are fit parameters. Inset: Temperature dependencies of $4\pi\chi'$ measured before (Curve 1) and after (Curve 2) the sample exposure to room temperature. The measurements were performed at $\nu = 5.4\,$kHz, $H_{ac} = 0.6\,$Oe, $H_{dc} = 0$.

performed according to the described measurement cycle.

Fig. 5 shows the temperature dependencies of $4\pi\chi'$ and $4\pi\chi''$ measured at frequencies from 0.312 to $20\,$kHz. One can see in Fig. 5 that T_c is essentially frequency-independent, unlike the shapes of the $4\pi\chi'(T)$ and $4\pi\chi''(T)$ responses to the phase transition, which change dramatically with the frequency.

Temperature dependencies of χ measured in a static magnetic field, H_{dc}, are shown in Fig. 6. According to Curves 1-3, an increase in H_{dc} suppresses the anomaly in $\chi(T)$. Increasing the driving ac field amplitude, H_{ac}, gives a similar effect as shown in Fig. 7.

In contrast to the ac susceptibility, the dc magnetization of the shock-wave pressure treated Mg/MgO-samples measured using a SQUID magnetometer in a standard zero-field-cooled and field-cooling regimes revealed no sign of the magnetic anomaly. At temperatures from 5 to $70\,$K, the sample was found non-magnetic, demonstrating a nearly temperature-independent magnetic moment $m \sim 10^{-6} - 10^{-5}$ e.m.u. in fields $H_{dc} = 30 - 300\,$Oe, respectively.

After completion of the ac susceptibility measurement series described above, the insert with the Mg/MgO-sample was finally removed from the cryostat and kept for $\approx 10\,$h at room temperature. The following χ measurements have shown, first of all, no time dependence of $\chi'(t)$ at $4.2\,$K, see Curve 2 in Fig. 4. Furthermore the T-dependence of χ' of the room-temperature-matured sample does not exhibit a step-like anomaly (see Curve 2 in the Inset of Fig. 4) and is independent on H_{ac} and H_{dc}, within the ranges used previously. Moreover, now
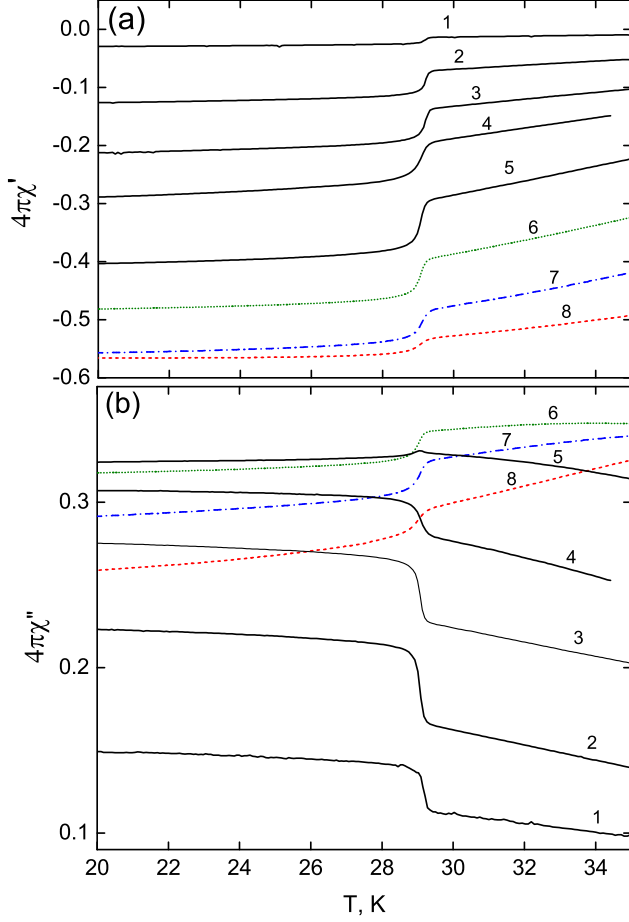
FIG. 5: Temperature dependencies of the real (a) and imaginary (b) parts of $4\pi\chi$ for the Mg/MgO-sample measured at frequencies 0.312, 0.923, 1.53, 3.12, 5.4, 7.69, 10 and 20 kHz (Curves 1 to 8, respectively). $H_{ac} = 0.6$ Oe, $H_{dc} = 0$.
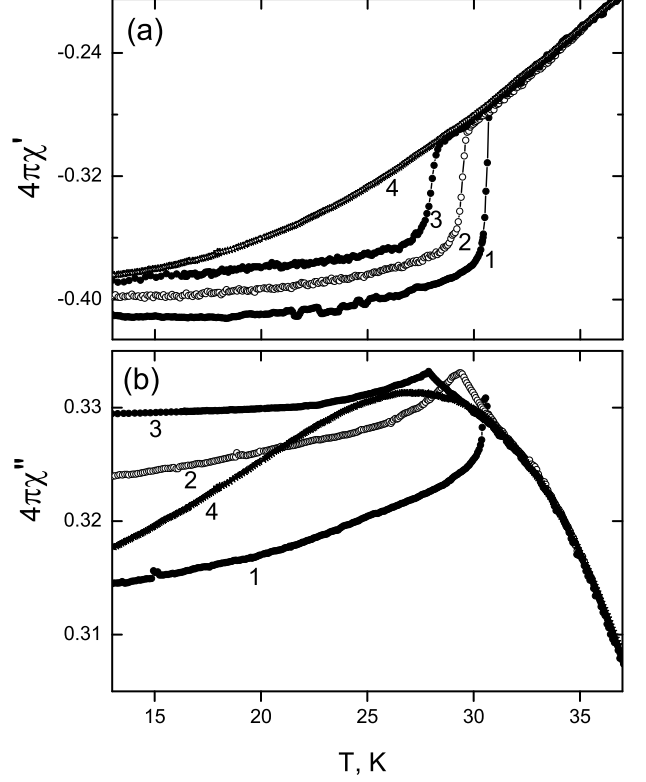

FIG. 6: Temperature dependencies of the real (a) and the imaginary (b) parts of $4\pi\chi$ for the Mg/MgO-sample measured under the dc magnetic field $H_{dc} = 0$, 84 Oe and 168 Oe (Curves 1 to 3, respectively). Curves 4 correspond to the same sample exposed for 10 hours to room temperature. The measurements were performed at $\nu = 5.4$ kHz in $H_{ac} = 0.23$ Oe.

$4\pi\chi'(T)$ and $4\pi\chi''(T)$ (Curve 2 in the Inset of Fig. 4, Curves 4 in Fig. 6 and Curves 5 in Fig. 7) practically coincide with those of pure magnesium sample subjected to the shock-wave pressure treatment under the same conditions. This denotes that the phase, which appeared in the Mg/MgO-sample during the shock-wave pressure treatment and which is responsible for the described anomalies in $\chi(T)$, is unstable at room temperature.

IV. DISCUSSION

A. Evidence of metastable superconductivity

We first focus on the sharp drop in $\chi'(T)$ observed in the shock-wave pressure treated Mg/MgO-sample at $T_c = 29$ K (Curve 1 in the Inset of Fig. 4), accompanied by a sharp anomaly in $4\pi\chi''(T)$ (Fig. 5). The response to the ac magnetic field is a function of the skin depth, $\delta \propto 1/\sqrt{\sigma\mu\nu}$, where σ is the conductivity and μ is the magnetic permeability of the material. According to the dc magnetization measurements, the Mg/MgO-samples are nonmagnetic ($\mu \sim 1$) showing no anomalies in the range 5-70 K. Therefore, the only reason for the observed change in $\chi'(T)$ is the temperature dependence of the electric conductivity of the sample. The observed drop in $\chi'(T)$ denotes that the conductivity rises steeply at $T_c \approx 29$ K as the temperature decreases, and we suppose that this is a superconducting transition.

This assumption is supported by the observed field dependencies of the anomaly in $\chi(T)$. The $\chi(T)$ measurements in a static magnetic field, H_{dc}, demonstrated the suppression of the $\chi(T)$ anomaly observed at $T_c \approx 30$ K, $H_{ac} = 0.23$ Oe, $H_{dc} = 0$ Oe, both in size and in the transition temperature, with increasing H_{dc} (Curves 1-3 in Fig. 6). Increasing the amplitude of the excitation field, H_{ac}, gives a similar effect, see Curves 1-4 in Fig. 7. The $\chi'(T)$ and $\chi''(T)$ dependencies presented in Figs. 6 and 7 are typical for superconducting materials[32,33] which implies a superconducting transition in the Mg/MgO sample.

None of the constituents of the sample, neither metallic Mg nor MgO are superconductors in the bulk. More-
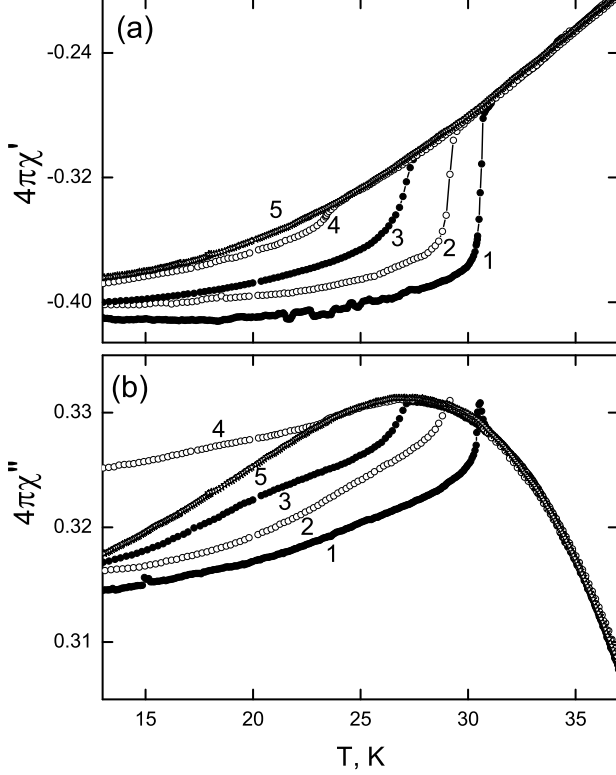
FIG. 7: Temperature dependencies of the real (a) and the imaginary (b) parts of $4\pi\chi$ for the Mg/MgO-sample measured with the amplitude of the ac driving field $H_{ac} = 0.23$, $0.6\,\mathrm{Oe}$, $1.5\,\mathrm{Oe}$ and $3.78\,\mathrm{Oe}$ (Curves 1 to 4, respectively). Curves 5 correspond to the same sample exposed for 10 h to room temperature. The measurements were performed at $\nu = 5.4\,\mathrm{kHz}$ in $H_{dc} = 0$.

over, none of them taken separately and subjected to the shock-wave pressure treatment under the same conditions, demonstrate any anomaly in $\chi(T)$. We believe therefore that the superconductivity in the shock-wave treated Mg/MgO sample is related to the interfacial layer formed between MgO and metallic Mg phases.

According to the results of both the ac susceptibility and the dc magnetization measurements, the superconducting interface in the Mg/MgO-sample does not form a closed superconducting surface capable of trapping the magnetic flux and keeping it constant, but rather consists of weakly linked granular superconducting two-dimensional islands.

First of all, that explains why the superconducting response is not detectable in the zero-field-cooled regime of the dc magnetization measurement, owing to the rapid decay of the surface shielding current after applying the dc magnetic field. On the contrary, in the ac mode the alternating magnetic field maintains the shielding current enabling to detect superconductivity even in discontinuous, energy dissipative superconducting loops formed by small, compared to the London penetration depth,

weakly linked superconducting clusters.

Secondly, at temperatures well below T_c, $4\pi\chi'(T) > -1$ and $\chi''(T) > 0$ (Figs. 5 - 7) which indicates an imperfect ac shielding, because a closed superconducting surface assumes $4\pi\chi'(T) = -1$ and $\chi''(T) = 0$. Non-zero χ'' at $T \ll T_c$ means that the superconductivity in the Mg/MgO-sample is accompanied by energy dissipation, which may take place in a granular superconducting structure due to inter- and intra-grain flux motions. Besides, systematic Y-axis shift of the $\chi''(T)$ with frequency (Fig. 5 (b)) reveals a considerable normal current contribution to the energy dissipation due to partial penetration of the ac magnetic field into the metallic magnesium core of the sample.

We believe therefore that the superconductivity in the Mg/MgO interfacial layer is formed by thin, compared to the London penetration depth λ, superconducting islands embedded into a non-superconducting host matrix and weakly coupled to each other by the proximity effect (if the host is metallic magnesium) or Josephson tunnelling (for the MgO host).

A typical elemental distribution at the Mg/MgO-interface is shown in Fig. 8. Substantial change of magnesium and oxygen concentrations is observed in the range of $\sim 2\,\mu$m, representing the thickness of the interface layer where the superconductivity occurs.

As it was mentioned above, the superconductivity of the Mg/MgO-sample is unstable at room temperature. The instability manifests itself as a decay of the superconducting transition after a 10-hour exposure of the vacuum-encapsulated sample to room temperature
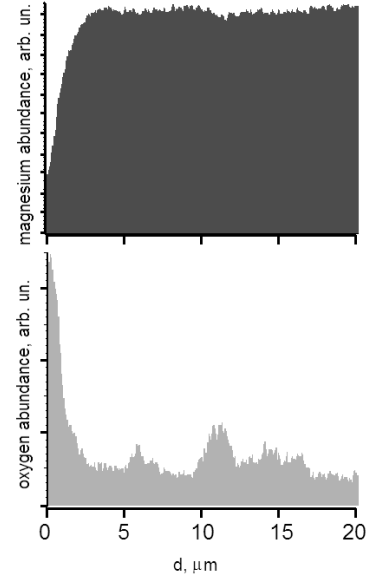

FIG. 8: Depth distributions of magnesium and oxygen contents in the shock-wave pressure treated Mg/MgO-sample. Substantial change of magnesium and oxygen concentrations is observed in the range of $\sim 2\,\mu$m from the sample surface ($d = 0$) demonstrating the interfacial Mg/MgO layer depth.

(Figs. 6 and 7), as well as vanishing of the time relaxation process of the ac susceptibility at $4.2\,\mathrm{K}$ (Fig. 4). The reason for such instability is apparently the oxygen/magnesium ionic diffusion processes activated at room temperature in the Mg/MgO interface, which destroy the superconducting interface.

The T-dependencies of $4\pi\chi'$ and $4\pi\chi''$ measured on the degraded Mg/MgO-sample (Curves 4 in Fig. 6 and Curves 5 in Fig. 7) are typical for normal nonmagnetic metals. Namely, at room temperature the skin depth, δ, of the ac magnetic field at $5.4\,\mathrm{kHz}$ in magnesium is $\approx 1.4\,\mathrm{mm}$, which is bigger than the sample thickness $d \approx 0.9\,\mathrm{mm}$. As the temperature decreases, the electric conductivity of the sample increases monotonically that leads to a decrease in δ, thus to a monotonic decrease in $\chi'(T)$.[34] At low temperatures, the electric conductivity of the sample becomes more flat in temperature, and $\chi'(T)$ sets constant.

In turn, χ'' characterizes the energy dissipation of the ac magnetic field in the sample, which is also a function of δ. The energy dissipation is low at $\delta \ll r$ (high-conductivity metal) and $\delta \gg r$ (insulator), where r is the sample depth. In the intermediate region $\chi''(T)$ has a maximum at $\delta \sim r$.[34] This broad maximum is seen on Curve 4 in Fig. 6 (b) and Curve 5 in Fig. 7 (b) at $T \approx 27\,\mathrm{K}$.

B. Superconductive glass

In a granular superconductor, positional disorder of individual superconducting grains introduces randomness and frustration into the system, resulting in a glassy behavior of the system.[35,36] In our experiments, the glassy behavior of the Mg/MgO-sample is evident from the observed slow dynamics of $\chi'(t)$ relaxation into the lower-energy diamagnetic ground state at $4.2\,\mathrm{K}$ (Fig. 4). The relaxation time, $\tau = 19.9\,\mathrm{min}$, was found frequency-independent in the range $312\,\mathrm{Hz}$ – $20\,\mathrm{kHz}$. The insensibility of τ to the excitation frequency is presumably a consequence of a significant time-scale mismatch between the $\chi'(t)$ relaxation process and the ac magnetic field oscillation period, $\tau \gg 1/2\pi\nu$: the field oscillations are too fast compared to τ to significantly influence the $\chi'(t)$ process.

The origin of such a long $\chi'(t)$ relaxation process is rather puzzling. It should be related to the granular structure of the superconducting Mg/MgO-interface formed by thin, compared to λ, superconducting islands weakly coupled to each other. However, no clear predictions concerning this dynamics of $\chi'(t)$ in a weak ac magnetic field exist on the basis of approaches involving collective creep or vortex-glass theories,[36] or any of the different models including the critical-state, superconducting-loop and superconducting-glass models.[33,35–38]

Unlike τ and T_c, the value of the ac susceptibility is strongly dependent on the frequency of the drive field. As

one can see in Fig. 5 (a), the $4\pi\chi'(T)$ plot shifts towards stronger diamagnetism with increasing the frequency, denoting a considerable contribution of the normal current component to χ' even at $T < T_c$. This contribution is presumably related to weak links such as intergrain boundaries separating the superconducting grains, as well as to normal currents induced in the metallic core of the sample due to partial penetration of the ac field.

As one can see in Fig. 5 (a), the step in $\chi'(T)$ at $29\,\mathrm{K}$ becomes bigger as the driving frequency increases from 0.312 to $5.4\,\mathrm{kHz}$ (Curves 1-5) and diminishes with further frequency increase (Curves 6-8). This can be explained assuming a superposition of normal and superconducting shielding currents contributing to $\chi'(T)$ in the granular superconductor.

Consider first the $\chi'(T)$ response at $29\,\mathrm{K}$ diminishing with the frequency ($\nu \geq 5.4\,\mathrm{kHz}$, Curves 5-8 in Fig. 5 (a)). This effect is well known for bulk metallic superconductors: in a normal metal, increasing the ac magnetic field frequency leads to diminishing skin depth δ, hence a bigger diamagnetic signal. As a result, at high frequency the normal metal just above T_c is nearly as diamagnetic as the superconductor just below T_c which makes the superconducting transition indistinguishable in $\chi'(T)$.

On the other hand, the suggested granular structure of the superconducting Mg/MgO-interface assumes intergranular weak links which can be considered as electric capacitors connected in series into the shielding supercurrent loops. Obviously, the higher is frequency, the better the superconducting islands are linked, hence the stronger is the superconducting shielding. Apparently, this explains the growth of the $\chi'(T)$ response at $29\,\mathrm{K}$ at frequencies up to $5.4\,\mathrm{kHz}$ (Curves 1-5 in Fig. 5 (a)). The two competing contributions superimpose in the studied Mg/MgO-sample to give a maximum of the $\chi'(T)$ response to the superconducting transition at $\nu_0 = 5.4\,\mathrm{kHz}$.

The evolution of $\chi''(T)$ with frequency is even more complicated, see Fig. 5 (b). At frequencies lower than $\nu_0 = 5.4\,\mathrm{kHz}$ (Curves 1-4) $\chi''(T)$ exhibits a step-like rise at cooling below $T_c \approx 29\,\mathrm{K}$, while at higher frequencies (Curves 6-8) a step-like drop is observed instead. At the crossover frequency ν_0 (Curve 5) a cusp-like anomaly is observed at T_c.

A possible explanation to such frequency behavior of $\chi''(T)$ which reflects energy dissipation in the system, is vortex dynamics influenced by the ac drive field.[36] We assume that the crossover frequency $\nu_0 = 5.4\,\mathrm{kHz}$ matches the vortex system relaxation rate $1/\tau_0$, $2\pi\nu_0\tau_0 = 1$. At low frequencies $\nu \ll \nu_0$, the ac field oscillations are slow compared to the vortex relaxation time τ_0, which enables the vortices respond to variation of the field. This gives rise to energy dissipative vortex motion, reflected in a step-like increase of $\chi''(T)$ upon cooling through $T_c \approx 29\,\mathrm{K}$ (Curves 1-4 in Fig. 5 (b)). At high frequencies $\nu \gg \nu_0$, the drive field oscillates too fast to disturb the vortex system which disables the energy dissipation through vortex motion. As a result, a step-like decrease of $\chi''(T)$ is observed upon cooling through $T_c \approx 29\,\mathrm{K}$

(Curves 6-8 in Fig. 5 (b)), which reflects shielding of the energy-dissipative interior of the sample by the supercurrents.

C. Nature of the Observed Superconductivity

None of the constituents of the sample, neither metallic Mg nor MgO are superconductors in the bulk. Moreover, none of them taken separately and subjected to the shock-wave pressure treatment under the same conditions, demonstrate any anomaly in $\chi(T)$. We believe therefore that the superconductivity in the shock-wave treated Mg/MgO sample is related to the interfacial layer formed between MgO and metallic Mg phases.

Unlike the $\chi(T)$ dependencies that change dramatically after exposing the sample to room temperature due to decay of the superconducting fraction, no change has been detected in the X-ray diffraction patterns of the Mg/MgO-sample after the room-temperature exposure. The fraction of the superconducting phase is therefore too small to be detected by the X-ray diffraction technique.

One may reasonably suggest ascribing the superconductivity in the Mg/MgO sample to some unknown superconducting magnesium oxide phase(s), unstable under normal conditions. However, this phenomenon has been discovered for other similar objects based on metals of various groups and their oxides (Na/NaO_x, Cu/CuO_x, Al/Al_2O_3 and Fe/FeO_x).[39–42] This indicates the generality of the observed phenomenon, rather than a unique property of Mg/MgO-system.

Alternatively, consider nanometer-sized metallic clusters which may spontaneously arise in the metal-oxide interface layer. Delocalized electrons of such cluster form energy shells similar to those in atoms or nuclei. Under specific conditions providing narrow, partially filled energy band at the Fermi level, superconducting pairing in such objects is expected to become very strong, forming a new hypothetical family of high-T_c (>150 K) superconductors.[43]

Besides, superconducting two-dimensional metal/oxide interfacial regions of sub-micron size may spontaneously arise in a relatively thick ($\sim 1\,\mu m$) boundary layer separating the metal and its oxide. In such interfaces which play a role of asymmetric confining potentials in the system of free electrons, the lack of spatial inversion symmetry may result in a topological change of the Fermi surface due to the spin-orbit splitting,[44] and lead to the enhanced superconductivity.

V. ACKNOWLEDGEMENTS

[1] H. Y. Hwang, Y. Iwasa, M. Kawasaki, B. Keimer, N. Nagaosa and Y. Tokure, Nature **11**, 103 (2012).

[2] J. Pereiro, A. Petrovic, C. Panagopoulosa and I. Bozovic, Physics Express **1**, 208 (2011).

[3] S. Gariglio and J. M. Triscone, C. R. Physique **12**, 591 (2011).

[4] N. V. Zavaritsky, Dokl. Akad. Nauk SSSR **86**, 501 (1952).

[5] V. Buckel and R. Hilsch, Z. Phys. **138**, 109 (1954).

[6] M. Strongin, O. F. Kammerer, D. H. Douglass, Jr. and M. H. Cohen, Phys. Rev. Lett. **19**, 121 (1967).

[7] M. Strongin, O. F. Kammerer, J. E. Crow, R. D. Parks, D. H. Douglass, Jr. and M. A. Jensen, Phys. Rev. Lett. **21**, 1320 (1968).

[8] M. Strongin and O. F. Kammerer, J. Appl. Phys. **8**, 2509 (1968).

[9] J. J. Hauser, Phys. Rev. B. **3**, 1611 (1971).

[10] G. J. H. M. Rijnders, G. Koster, D. H. A. Blank, and H. Rogalla, Appl. Phys. Lett. **70**, 1888 (1997).

[11] G. Logvenov, A. Gozar, and I. Bozovic, Science **326**, 699 (2009).

[12] K. Murase, S. Ishida, S. Takaoka, T. Okumura, H. Fujiyasu, A. Ishida and M. Aoki, Surf. Sci. **170**, 486 (1986).

[13] O. A. Mironov, B. A. Svitskii, A. Yu. Sipatov, A. I. Fedorenko, A. N. Chirkin, S. V. Chistyakov and L. P. Shpakovskaya, Sov. Phys. JETP **48**, 106 (1988).

[14] M. Strongin, J. Supercond. **4**, 357 (1991).

[15] N Ya. Fogel, E. I. Buchstab, Yu. V. Bomze, O. I. Yuzephovich, A. Yu. Sipatov, E. A. Pashitskii, A. Danilov, V. Langer, R. I. Shekhter and M. Jonson,Phys. Rev. B **66**, 174513 (2002).

[16] N. Reyren, S. Thiel, A. D. Caviglia, L. F. Kourkoutis, G. Hammerl, C. Richter, C. W. Schneider, T. Kopp, A-S. Rüetschi, D. Jaccard, M. Gabay, D. A. Muller, J-M. Triscone and J. Mannhart, Science **317**, 1196 (2007).

[17] N. Reyren, S. Gariglio, A. D. Caviglia, D. Jaccard, T. Schneider and J. M. Triscone, Appl. Phys. Lett. **94**, 112506 (2009).

[18] A. Gozar, G. Logvenov, L. Fitting Kourkoutis, A. T. Bollinger, L. A. Giannuzzi, D. A. Muller, and I. Bozovic, Nature **455**, 782 (2008).

[19] N. S. Sidorov, A. V. Palnichenko and S. S. Khasanov, Solid State Commun. **152**, 443 (2012).

[20] N. S. Sidorov, A. V. Palnichenko and O. M. Vyaselev, Physica C **480**, 123 (2012).

[21] A. V. Palnichenko, O. M. Vyaselev and N. S. Sidorov, JETP Lett.**86**, 272 (2007).

[22] Ya. B. Zeldovich and Yu. P. Raizer, *Physics of Shock Waves and High Temperature Hydrodynamics Phenomena* (Academic Press, New York, 1966).

[23] G. I. Kanel', A. M. Molodets and A. A. Vorob'ev, Com-

bustion, Explosion, and Shock Waves **10**, 793 (1974).

[24] V. E. Fortov, Physics-Uspekhi **50**, 333 (2007).

[25] Yu. A. Ossipyan, N. S. Sidorov, A. V. Palnichenko, O. M. Vyaselev, M. V. Kartsovnik M. Opel, V. V. Avdonin, D. V. Shakhrai, N. V. Biktimirova and A. A. Golyshev, Chem. Phys. Lett. **457**, 74 (2008).

[26] N. S. Sidorov, A. V. Palnichenko, V. V. Avdonin, D. V. Shakhrai, O. G. Rybchenko, S. S. Khasanov and M. K. Sakharov, Solid State Commun. **150** 1108 (2010).

[27] P. I. Dorogokupets, Phys. Chem. Minerals, **37** 677 (2010).

[28] *Shock Wave Database*, internet available: http://www.ficp.ac.ru/rusbank.

[29] D. -X. Chen and V. Skumryev, Rev. Sci. Instrum, **81** 025104 (2010).

[30] *The International Centre for Diffraction Data (JCPDS), 2008*, Iinternet available: http://www.icdd.com/products/2008SalesCatalog.pdf.

[31] *Spin Glasses and Random Fields*, edited by A. P. Young (World Scientific, Singapore, 1998).

[32] R. A. Hein, Phys. Rev. B **33** 7539 (1986).

[33] T. Ishida and R. B. Goldfarb, Phys. Rev. B **41** 8937 (1990).

[34] L D. Landau and E. M. Lifshitz, *Course of Theoretical Physics, Vol. 8: Electrodynamics of Continuous Media* (Nauka, Moscow, 1982; Pergamon, New York, 1984).

[35] C. Ebner and D. Stroud, Phys. Rev. B **31** 165 (1985).

[36] G. Blatter, M. Y. Feigel'man, Y. B. Geshkenbein, A. I. Larkin and V. M. Vinokur, Rev. Mod. Phys. **66** 1125 (1994).

[37] H. Kawamura and M. S. Li, Phys. Rev. B **54** 619 (1996).

[38] A. P. Young, Physica B **321** 183 (2002).

[39] N. S. Sidorov, A. V. Palnichenko and S. S. Khasanov, Solid State Commun. **150** 1483 (2010).

[40] N. S. Sidorov, A. V. Palnichenko and S. S. Khasanov, Phys. C. **471** 247 (2011).

[41] N. S. Sidorov, A. V. Palnichenko and S. S. Khasanov, JETP. Lett. **94** 134 (2011).

[42] N. S. Sidorov, A. V. Palnichenko and I. I. Zver'kova, Phys. C. **471** 406 (2011).

[43] V. Z. Kresin and Yu. N. Ovchinnikov, Usp. Fiz. Nauk **178** 449 (2008).

[44] E. Cappelluti, C. Grimaldi and F. Marsiglio, Phys. Rev. Lett. **98** 167002 (2007).